Field-Inhomogeneity-Corrected Low-Rank Filtering of Magnetic Resonance Spectroscopic Imaging Data

Yan Liu[1] *Member, IEEE*, Chao Ma[2] *Member, IEEE*, Bryan Clifford[3] *Student Member, IEEE*, Fan Lam[3] *Student Member, IEEE*, Curtis L. Johnson[2] *Member, IEEE*, Zhi-Pei Liang[3] *Fellow, IEEE*

***Abstract*— Low signal-to-noise ratio has been a major problem in magnetic resonance spectroscopic imaging (MRSI). A low-rank approximation based denoising method has been recently proposed to address this problem by exploiting the partial separability properties of MRSI data. However, field inhomogeneity, an unavoidable complication in practice, can violate the partial separability assumption and thus degrade the denoising performance of the low-rank filtering method. This paper presents a field-inhomogeneity-corrected low-rank filtering method to achieve more robust denoising of practical MRSI data. In vivo experiment results have been used to demonstrate the effectiveness of the proposed method.**

I. INTRODUCTION

The concentration levels of metabolites of the brain, e.g., N-acetylaspartate (NAA), Choline (Cho) and Creatine (Cr), provide important information about neuronal viability, cellular membrane synthesis and energy production [1], [2], [3]. Magnetic resonance spectroscopic imaging (MRSI) [4], [5], [6] is so far the only non-invasive way to map the concentrations of these metabolites, however, its potential in clinical and research applications has not yet been fully exploited. A key challenge of using MRSI in practice is signal-to-noise ratio (SNR), which is fundamentally limited by the sensitivity of nuclear magnetic resonance (NMR) phenomena and the concentrations of brain metabolites.

A straightforward way to improve SNR is signal averaging, which can be done temporally by repeating experiments multiple times or spatially by applying smooth filters. However, such methods compromise the already long data acquisition time and the already low resolution of MRSI. A better way is to do denoising using the underlying properties of the signal. Many signal models have been proposed for general denoising applications, including those based on wavelet representations [7], PDEs [8] and sparsity representations [9]. Most recently, the partial separability (PS) model [10], which results in low-rank data, has been exploited for denoising in MRI [11], [12]. Especially, the LORA (low-rank approximation) method has been proposed to denoising MRSI data and reported superior performance compared to the conventional methods [12].

However, non-negligible field inhomogeneity effects in practical MRSI data can violate the PS assumption (i.e., resulting in significantly increased rank) and degrade the denoising performance of LORA. In this paper, we propose a field-inhomogeneity-corrected low-rank filtering approach to address this issue. More specifically, the proposed method first corrects the field inhomogeneity effects using a high-resolution field map and prior edge information (derived from high-resolution reference images) and then calculates a low-rank approximation of the corrected data for denoising. We demonstrate the effectiveness of the proposed method using in vivo MRSI data acquired on a 3.0 T scanner.

The rest of the paper is organized as follows: Section II briefly reviews LORA; Section III describes the proposed method; Section IV presents representative denoising results using in vivo experiment data, followed by the conclusion of this paper in Section V.

II. BACKGROUND

In the absence of field inhomogeneity, the acquired (k,t)-space data can be expressed as

$$s(\mathbf{k},t) = \int \rho(\mathbf{r},t) e^{-i2\pi \mathbf{k}\cdot\mathbf{r}} d\mathbf{r} + \varepsilon(\mathbf{k},t), \tag{1}$$

where $\rho(\mathbf{r},t)$ denotes the desired spatial-temporal function of the metabolite signal, and $\varepsilon(\mathbf{k},t)$ is the measurement noise, which is assumed to be a complex white Gaussian noise.

In LORA, $\rho(\mathbf{r},t)$ is modeled by low-order PS functions [10], [12]:

$$\rho(\mathbf{r},t) = \sum_{l=1}^{L} a_l(\mathbf{r})\psi_l(t), \tag{2}$$

where $a_l(\mathbf{r})$ is the l-th spatial basis function, $\psi_l(t)$ is the corresponding temporal basis function, and L is the model order. The validity of the PS model in (2) for MRSI data has been discussed in [12].

It is well known that data satisfying the PS model has a low-rank structure [10]. More specifically, suppose the measured data are $\{s(\mathbf{k}_n,t_m)\}_{n,m=1}^{N,M}$, where N and M denote the number of spatial and spectral encodings, respectively.

* The work presented in this paper was supported in part by research grant 41306203 National Natural Science Foundation of China (Y. Liu) and by a Beckman Postdoctoral Fellowship (C. Ma).

[1]Y. Liu is with the University of Chinese Academy of Sciences,Beijing 100049, China. Y. Liu now is a visiting scholar in the Beckman Institute for Advanced Science and Technology, University of Illinois, at Urbana-Champaign, Urbana, IL, 61801 (email:yanliu@ucas.ac.cn).

[2]C. Ma and C. L. Johnson are with the Beckman Institute for Advanced Science and Technology, University of Illinois, at Urbana-Champaign, Urbana, IL, 61801.

[3]B. Clifford, F. Lam and Z.-P. Liang are with the Department of Electrical and Computer Engineering and Backman Institute for Advanced Science and Technology, University of Illinois at Urbana-Champaign, 1406 West Green Street, Urbana, IL, 61801.

978-1-4244-7929-0/14/$26.00 ©2014 IEEE

The corresponding Casorati matrix can be formed as:

$$\mathbf{C} = \begin{bmatrix} s(\mathbf{k}_1,t_1) & s(\mathbf{k}_1,t_2) & \cdots & s(\mathbf{k}_1,t_M) \\ s(\mathbf{k}_2,t_1) & s(\mathbf{k}_2,t_2) & \cdots & s(\mathbf{k}_2,t_M) \\ \vdots & \vdots & \ddots & \vdots \\ s(\mathbf{k}_N,t_1) & s(\mathbf{k}_N,t_2) & \cdots & s(\mathbf{k}_N,t_M) \end{bmatrix}, \quad (3)$$

In the noiseless case, the PS model in Eq. (2) makes the rank of the Casorati matrix in Eq. (3) upper-bounded by L [10], [12], which can be much smaller than the dimension N and M in practice.

In the noisy case, the Casorati matrix becomes full rank. We then seek an optimal low-rank (rank L) approximation of the Casorati matrix for denoising:

$$\begin{aligned} \mathbf{C}^* = \quad & \underset{\hat{\mathbf{C}}}{\operatorname{argmin}} \quad \| \mathbf{C} - \hat{\mathbf{C}} \|_{\mathrm{F}}^2, \\ & \text{s.t.} \qquad \operatorname{rank}(\hat{\mathbf{C}}) = L, \end{aligned} \quad (4)$$

where $\| \cdot \|_{\mathrm{F}}$ denotes the Frobenius norm.

The solution of (4) can be obtained by calculating the singular value decomposition (SVD) of the Casorati matrix $\mathbf{C}$:

$$\mathbf{C}^* = \sum_{l=1}^{L} \sigma_l \mathbf{u}_l \mathbf{v}_l^{\mathrm{H}}, \quad (5)$$

where σ_l, $\mathbf{u}_l$, and $\mathbf{v}_l$ are the l-th singular value, left and right singular vector of $\mathbf{C}$. Taking the discrete Fourier transform (DFT) along each column of $\mathbf{C}^*$ yields the denoised MRSI reconstruction.

III. FIELD-INHOMOGENEITY-CORRECTED LOW-RANK FILTERING

In practice, field inhomogeneity is caused by imperfections of the main magnetic field of an MRI scanner and by inhomogeneous magnetic susceptibilities of tissues [13], [14], [15]. In the presence of field inhomogeneity, the MRSI signal becomes

$$\tilde{s}(\mathbf{k},t) = \int \tilde{\rho}(\mathbf{r},t) e^{-i2\pi \mathbf{k}\cdot\mathbf{r}} d\mathbf{r} + \varepsilon(\mathbf{k},t), \quad (6)$$

where $\tilde{\rho}(\mathbf{r},t)$ contains an additional phase term caused by field inhomogeneity:

$$\tilde{\rho}(\mathbf{r},t) = \rho(\mathbf{r},t) e^{-i2\pi\Delta f(\mathbf{r})t}, \quad (7)$$

$\Delta f(\mathbf{r})$ denotes field inhomogeneity in Hertz.

Since the phase term $e^{-i2\pi\Delta f(\mathbf{r})t}$ in (7) is not a separable function, $\tilde{\rho}(\mathbf{r},t)$ in (7) cannot be represented by PS functions as $\rho(\mathbf{r},t)$ in (2). Consequently, the corresponding Casorati matrix of $\tilde{s}(\mathbf{k},t)$ in (6) does not have a low-rank structure in the noiseless case. Therefore, the field inhomogeneity effects should be removed before applying LORA for denoising.

A high-resolution field map can be easily acquired in an MRSI experiment. If the MRSI data have the same resolution, the field inhomogeneity correction can be easily done by first performing DFT to the measured data to get a high-resolution spatial-temporal data and then correcting the field inhomogeneity induced phase accordingly. This method is often known as the conjugate phase (CP) method [16]. However, limited k-space data are often acquired in the conventional MRSI methods due to experimental time constraints. The challenge is to correct the field inhomogeneity effects with limited k-space data. For instance, the CP method can suffer from the partial volume effects in the case of limited k-space data.

In this paper, we use a different approach to correct the field inhomogeneity effects with limited k-space data. We aim to reconstruct a high-resolution MRSI data from limited k-space data by incorporating edge information derived from high resolution anatomical reference images. The CP method is then used to correct the field inhomogeneity effects. The corrected high-resolution data is truncated in k-space to obtain low-resolution but filed-inhomogeneity-corrected data. Finally, LORA is applied to the corrected data for denoising. Note that the high-resolution MRSI reconstruction only serves as an intermediate result. It has also been shown in [17], [18] that incorporating edge information has additional denoising effects on the MRSI data.

Mathematically, we perform field inhomogeneity correction by solving the following least-square problem with a weighted ℓ_2-norm penalty [19]:

$$\rho_c = \underset{\rho}{\operatorname{argmin}} \| \Omega\mathbf{F}\mathbf{B}\rho - \mathbf{s} \|_2^2 + \lambda \| \mathbf{D}\rho \|_2^2 . \quad (8)$$

In (8), Ω is a k-space sampling operator, $\mathbf{F}$ is a DFT matrix, $\mathbf{B}$ is a phase term caused by the field inhomogeneity, ρ is a vector representing the discretized spatial-temporal function, $\mathbf{s}$ is a vector representing the measured (k,t)-space data, λ is a regularization parameter, which can be selected using the discrepancy principle, and the weighted ℓ_2-norm penalty term is defined by

$$\| \mathbf{D}\rho \|_2^2 = \sum_{n_t} \sum_{n_1} \sum_{n_2 \in P_{n_1}} w_{n_1,n_2} |\rho_{n_1,n_t} - \rho_{n_2,n_t}|^2, \quad (9)$$

where P_{n_1} is the eight-pixel neighborhood of voxel n_1 and w_{n_1,n_2} is the weighting coefficient derived from high resolution reference images. Intuitively, the weights are introduced to penalize spatial smoothness while preserving edges: large weights in smooth regions yielding strong smoothness penalties and small weights across edges yielding weak smoothness penalties. For more details on how to determine w_{n_1,n_2} see [17].

Equation (8) can be efficiently solved by solving the following normal equation using the conjugate gradient method:

$$(\mathbf{B}^{\mathrm{H}}\mathbf{F}^{\mathrm{H}}\Omega^{\mathrm{H}}\Omega\mathbf{F}\mathbf{B} + \lambda\mathbf{D}^{\mathrm{H}}\mathbf{D})\rho_c = \mathbf{B}^{\mathrm{H}}\mathbf{F}^{\mathrm{H}}\Omega^{\mathrm{H}}\mathbf{s}. \quad (10)$$

Field inhomogeneity corrected data is then obtained by

$$\mathbf{s}_c = \Omega\mathbf{F}\rho_c. \quad (11)$$

The Casorati matrix can be formed accordingly and followed by applying LORA for denoising.

IV. RESULTS

A. In vivo experiments

Experimental data were acquired from a healthy volunteer on a 3.0 T Siemens Trio scanner. The study was conducted

in compliance with the regulations of the local institutional board. A PRESS-CSI sequence was used to acquire MRSI data with CHESS pulses for water suppression and eight outer-volume-suppression bands for fat suppression (Fig. 1(a). The remaining imaging parameters were: TE = 130 ms, TR = 1000 ms, bandwidth = 2000 Hz, 20×20 encoding matrix (elliptical sampling). A high resolution field map was acquired using the scanner built-in field mapping sequence with a 128×128 encoding matrix (Fig. 1(b). Two spin-echo images were acquired with the same resolution with 130/1200 ms and 30/1200 ms TE/TR, respectively, which served as reference anatomical images (Fig. 1(c) and 1(d). In addition, a three-point Dixon method was used to acquire water and fat images also at the same resolution.

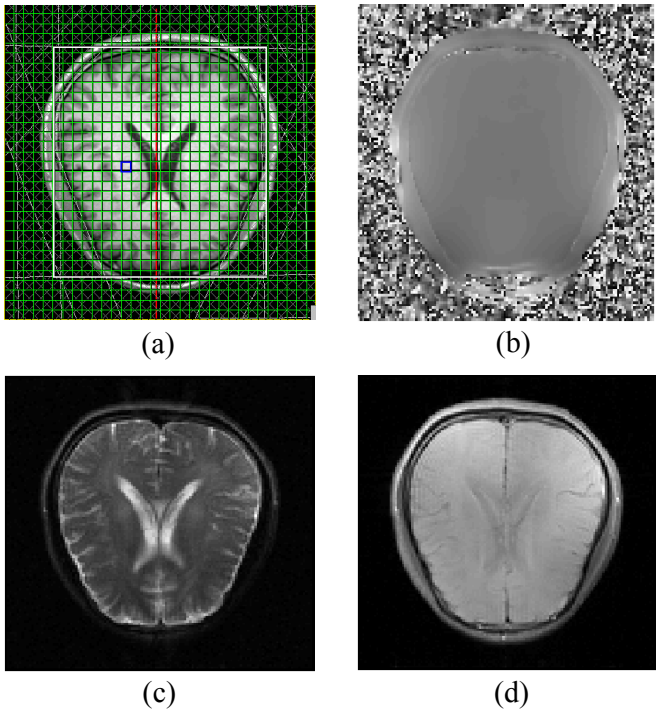

Fig. 1. In vivo experiment setup. (a) Slice and outer-volume-saturation bands positions in the CSI experiment. (b) Field map. (c) and (d) Anatomical reference images.

B. Removal of nuisance signals

Although water and fat suppression can be quite effective in a CSI sequence, residual water and fat signals are still commonly found in the acquired MRSI data. These nuisance signals are of little interest but can be significantly larger than metabolite signals even with suppression due to the much higher concentrations of water and fat. The nuisance signals must be removed before denoising using the proposed method, otherwise the singular value distribution of the resulting Casorati matrix will be dominated by the contributions of the nuisance signals.

A HSVD based method was used to remove the residual water signals in a point-by-point fashion [20]. A recently proposed fat signal removal method was used to remove the residual fat signals, which was based on a spatial-spectral model of fat signals [21].

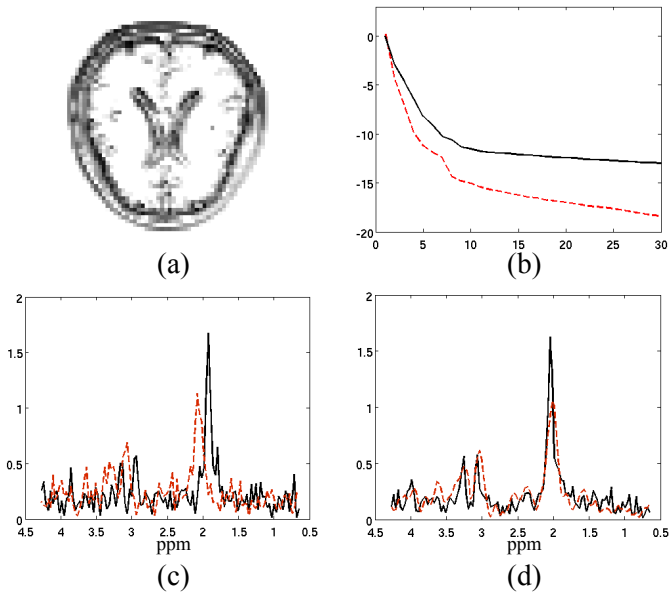

Fig. 2. Field inhomogeneity correction results. (a) Weights in (9), which were derived from Fig. 1(c) and 1(d). (b) Singular value distribution before (solid black line) and after (dashed red line) field inhomogeneity correction. (c) and (d) Representative spectra at two different locations before and after field inhomogeneity correction.

C. Denoising results

Field inhomogeneity correction results are shown in Fig. 2. Fig. 2(a) shows the weights in (9), which were derived from Fig. 1(c) and 1(d). Fig. 2(b) shows the singular value distribution of the MRSI data (Casorati matrix) before (black solid line) and after (red dashed line) field inhomogeneity correction. It can be clearly seen that field inhomogeneity correction made the singular values decay faster. In other words, field inhomogeneity correction promoted the low-rankness of the MRSI data as expected. Fig. 2(c) and 2(d) show representative spectra at two different locations before and after field inhomogeneity correction, respectively. Good alignment of spectra are found after field inhomogeneity correction. Comparing Fig. 2(d) with Fig. 2(c), noticeable denoising effects are also seen, which are the expected results of incorporating edge weights in (8).

Denoising results of the proposed method are shown in Fig. 3. Fig. 3(a) and 3(b) show a representative spectrum before and after denoising, respectively. The noise in the original spectrum has been significantly reduced. Fig. 3(c) and 3(d) show NAA maps before and after denoising. The maps were calculated by integrating spectrum around the NAA peak. After denoising, the ventricle structure (the center dark region in Fig. 3(d)), where low NAA concentrations are expected, can been better detected.

V. CONCLUSION

This paper presents a field-inhomogeneity-corrected low-rank filtering method to improve SNR of MRSI data. High-

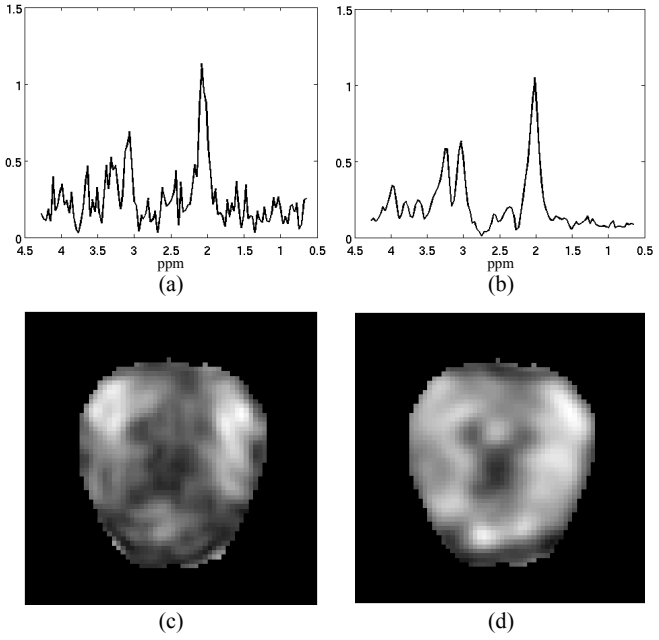

Fig. 3. Denoising results. (a) and (b) A representative spectrum before and after denoising. (c) and (d) NAA maps before and after denoising.

resolution field maps and a priori structural information from high-resolution reference images are used to correct the field inhomogeneity effects with limited k-space data. It promotes the low-rank structure of MRSI data for the following LORA denoising. In vivo experimental results have demonstrate that the proposed method can denoise MRSI data with low SNRs effectively. The proposed method may prove useful in high-resolution MRSI, where the SNR issue is particularly challenging.

REFERENCES

[1] R. A. de Graaf, *In vivo NMR spectroscopy: Principles and techniques*, John Wiley & Sons, Ltd, second edition, 2007.

[2] P. B. Barker and D. D. M. Lin, "In vivo proton MR spectroscopy of the human brain," *Prog. Nuclear Magn. Reson. Med.*, vol. 49, pp. 99-128, 2006.

[3] A. Henning, "In vivo 1H MRS applications," *Encyclopedia of Spectroscopy and Spectrometry*, J. C. Lindon, Ed., Amsterdam, Netherlands: Elsevier, 2010, pp. 1077-1084.

[4] P. C. Lauterbur, D. M. Kramer, W. V. House, and C. N. Chen, "Zeugmatographic high resolution nuclear magnetic resonance spectroscopy: images of chemical inhomogeneity within macroscopic objects," *J. Am. Chem. Soc.*, vol. 97, pp. 6866-6868, 1975.

[5] T. R. Brown, B. M. Kincaid, and K. Ugurbil, "NMR chemical shift imaging in three dimensions," *Proc. Nat. Acad. Sci.,* vol. 79, pp. 3523-3526, 1982.

[6] A. A. Maudsley, S. K. Hilal, W. H. Perman, and H. E. Simon,"Spatially resolved high resolution spectroscopy by four-dimensional NMR," *J. Magn. Reson.*, vol. 51, pp. 147-152, 1983.

[7] D. L. Donoho, "De-noising by soft-threshholding," *IEEE Trans Inf. Theory,* vol. 41, pp. 613-627, 1995.

[8] A. Buades, B. Coll and J. M. Morel, "A review of image denoising algorithms, with a new one," *Multiscale Model. Simul.*, vol. 4, pp. 490-530, 2005.

[9] M. Elad and M. Aharon, "Image denoising via sparse and redundant representations over learned dictionaries," *IEEE Trans. Imag. Process.*, vol. 15, pp. 3736-3745, 2006.

[10] Z.-P. Liang, "Spatiotemporal imaging with partially separable functions," *Proc. IEEE Intl. Symposium Biomed. Imag.*, 2007, pp. 988-991.

[11] F. Lam, S. D. Babacan, J. P. Haldar, M. W. Weiner, N. Schuff, and Z.-P. Liang, "Denoising diffusion-weighted magnitude MR images using rank and edge constraints," *Magn. Reson. Med.*, vol. 71, pp. 1272-1284, 2014.

[12] H. M. Nguyen, X. Peng, M. N. Do and Z.-P. Liang, "Denoising MR spectroscopic imaging data with low-rank approximations," *IEEE Trans. Biomedical Engineering*, vol. 60, pp. 78-89, 2013.

[13] A. Bashir and D. A. Yablonskiy, "Natural linewidth chemical shift imaging (NL-CSI)," *Magn. Reson. Med.*, vol. 56, pp. 7-18, 2006.

[14] I. Khalidov, D. Van De Ville, M. Jacob, F. Lazeyras, and M. Unser, "BSLIM: Spectral localization by imaging with explicit B_0 field inhomogeneity compensation," *IEEE Trans. Med. Imaging*, vol. 26, pp. 990-1000, 2007.

[15] M. E. Halse and P. T. Callaghan, "Imaged deconvolution: a method for extracting high-resolution NMR spectra from inhomogeneity fields," *J. Magn. Reson.*, vol.185, pp.130-137, 2007.

[16] D. C. Noll, J. A. Fessler and B. P. Sutton, "Conjugate phase MRI reconstruction with spatially variant sample density correction," *IEEE Trans. Med. Imaging*, vol 24, pp. 325-336, 2005.

[17] J. P. Haldar, D. Hernando, S. K. Song and Z.-P. Liang, "Anatomically constrained reconstruction from noisy data," *Magn. Reson. Med.*, vol. 59, pp. 810-818, 2008.

[18] H. M. Nguyen, J. P. Haldar, M. N. Do, and Z.-P. Liang, "Denoising of MR spectroscopic imaging data with spatial-spectral regularization," *Proc. IEEE Intl. Symposium Biomed. Imag.*, 2010, pp. 720-723.

[19] X. Peng, H. M. Hien, J. Haldar, D. Hernando, X.-P. Wang and Z.-P. Liang, "Correction of field inhomogeneity effects on limited k-space MRSI data using anatomical constraints," *Proc. 32nd Annual Intl. Meeting IEEE-EMBS*, 2010, pp. 883-886.

[20] A. van den Boogaart, D. van Ormondt, W. W. F. Pijnappel, R. de Beer R., and M. Ala-Korpela, "Removal of the water resonance from 1H magnetic resonance spectra," *Mathematics in Signal Processing III*, J. G. McWhirter, Ed., Oxford: Clarendon Press, 1994, pp. 175-195.

[21] C. Ma, F. Lam, C. Johnson and Z.-P. Liang, "Removal of nuisance lipid signals from limited k-space data in 1H MRSI of the brain," *Proc. Intl. Soc. Mag. Reson. Med.*, 2014, pp. 2887.